

Design of Highly Selective Dual Band Band Stop Filter using Dual-Path Step Impedance Resonator

Abdul Rehman¹, Muhammad Abdul Rehman¹, Nosheen Aziz², Bilal Mushtaq¹, Muhammad Jamshed Abbass¹, Sohail Khalid¹, and Ahmed Zubair Jan³

¹Faculty of Engineering and Applied Science Riphah International University Islamabad, Pakistan

²The Women University Multan, Pakistan

³Wroclaw University of science and Technology, Poland

Corresponding author: Abdul Rehman (e-mail: abdul.rehman03@hotmail.com).

Received: 15/04/2022, Revised: 20/07/2022, Accepted: 30/08/2022

Abstract- In this article, the primary focus is on improving selectivity through the design of a dual-band bandstop filter (BSF), which is the abbreviation for bandstop filter. For the design of the filter, a dual-path Step Impedance Resonator, or DP-SIR, is utilised. A theoretical analysis of the suggested DP-SIR structure is presented in this body of work. At 3.76 and 11.04 GHz, the proposed architecture produces a dual-band BSF with fractional bandwidths of 50.5% and 16.36%, respectively. The comprehensive study demonstrates that the resonant frequencies can be controlled by adjusting the electrical length of the SIR. In addition, it has been found that dual-path SIR is involved in the production of finite frequency transmission poles, which results in an improvement in selectivity. This was discovered by accident. The results of the measurements and the simulations are fairly consistent with one another.

Keywords—Bandstop filter, Step Impedance Resonator, Microwave.

I. INTRODUCTION

The evolution of sophisticated communication systems has increased the demand for high-quality RF microwave filters. The rising demand necessitates immediate action to optimise the use of an increasingly congested electromagnetic spectrum. The presence of spurious frequencies within a communication channel, on the other hand, poses a greater challenge. The quality of a bandstop filter is determined by some critical figures of merit (FOM). These include Passband Ripples, Stopband Attenuation, High Selectivity, Low Return Loss, and Group Delay. Various approaches have been offered to design a dual-band bandstop filter. In [1], a dual-bandstop response is achieved using bandstop resonators coupled with the transmission line. The proposed design has increased filter order, steep roll-off characteristics, and better narrow-band performance. In [2], DBBSF is realized by combining two different methodologies, i.e., Spurline and Stepped Impedance Resonators (SIRs), with electronically tuned Barium Strontium Titanate (BST) Capacitors. This novel filter provides two stopbands, which are independently tuned, thereby reducing size and cost. A compact dual-wideband bandstop filter with high isolation using open coupled lines and the transversal signal-interference concept is proposed in [3]. However, a third-order stopband with high selectivity and a wider upper passband has been realized. In [4], a Defected Microstrip Structure (DMS) based wideband bandstop filter is depicted with the main focus on reducing electromagnetic compatibility (EMC). In the illustrated structure, two wide-stopbands have been controlled using two identical DMS but different sizes. In [5], a four-notch dual-band bandstop filter is analyzed via an M-shaped DMS approach. The main

advantage is that the filter's frequency may be adjusted depending on changes to DMS parameters. Whereas fabrication difficulty is the main drawback of the DMS approach. In [6], a unique wideband bandstop filter design utilising a Defected Ground Structure (DGS) and a Stepped Impedance Resonator (SIR) is proposed.

By adjusting the impedance of the transmission line sections, the stopband's bandwidth can be changed. Moreover, the circuit is difficult to fabricate. A microstrip bandstop filter is discussed in [7] using varying electrical lengths of parallel-coupled microstrip lines. The reported design has provided higher selectivity, higher return loss, and low insertion loss in the passband. In [8], the dual-band Split Ring Resonator (SRR) methodology is demonstrated based on the bandwidth ratio model. It provides a good idea to control parameters simultaneously, such as resonant frequencies and bandwidth ratio, using unequal ring resonators. In [9], an open or short microstrip coupled line method is elaborated. In this design, the stopband frequencies are adjusted by changing the coupled lines' even or odd mode impedances. Similarly, in [10], the filter is understood by placing two symmetrical coupled line stubs whose points are shorted to get stopband characteristics. [11] proposes a compact bandstop filter with four transmission poles (TPs) made up of parallel-coupled lines and open stubs. Further, a DBBSF is provided in [12], using typical open stub resonators and embedding strip lines. One stripline is embedded between the line connecting the two open stubs, while the others are on the edge of the open stubs. Finally, a novel methodology is presented in [13] by cascading dual-coupled resonators to realize microstrip BSF with an arbitrarily short-through line.



This work is licensed under a Creative Commons Attribution 4.0 International License, which permits unrestricted use, distribution, and reproduction in any medium, provided the original work is properly cited.

- Doing so enables them to have an arbitrary phase shift between the adjacent cascaded sections without increasing the length of the transmission line.
- This paper illustrates an exact synthesis procedure. The dual-band bandstop filter topology is validated using the advanced synthesis technique.

Section II realizes the proposed topology based on an open stub-loaded ring resonator having a step impedance resonator (SIR). Instead of a uniform transmission line, SIR is suited to shorten the middle length, eventually achieving compactness. As opposed to this, adding SIR also results in bandstop behaviour, which muffles the spurious resonances at higher frequencies. Section III provides the simulation and results from the analysis. The comparison of results is also given in this section. Whereas section IV concludes the findings and rationale of the proposed filter design.

II. PROPOSED DUAL-BAND BANDSTOP FILTER

A. Design of Proposed Filter

Figure 1 (a) depicts the proposed transmission line structure, composed of Path 1 and Path 2 as the transmission paths. Path 1 entails an open-circuit stub hanging in between the Stepped-Impedance Resonators (SIR). However, from Fig. 1, path 2 entails a straight transmission line. An equivalent model of SIR; is also given in Fig.1 (b). The SIR is a transmission line resonator (TEM and quasi-TEM mode resonator) made of more than two transmission lines with various characteristic impedances [24]. An open-circuit stub (OCS) is represented as a resonator with a characteristic impedance. However, the electrical length of the transmission line and stub resonators at the designed frequency is.

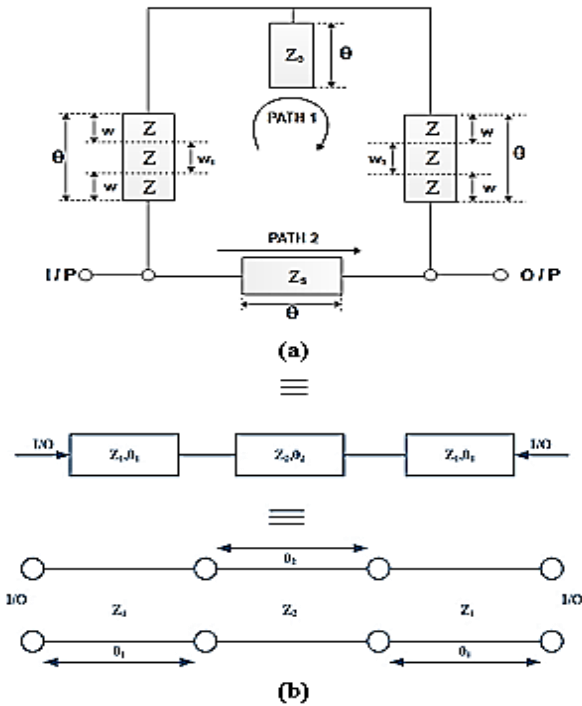


FIGURE 1: Ideal model design for DBBSF (b) SIR with three-step-impedance TL

B. Synthesis Analysis of Proposed Filter

The proposed filter design parameters are obtained by following the synthesis procedure with the ultimate goal of extracting the filtering function. The transmission coefficient parameter of the proposed filter is derived by translating ABCD parameters into Y-parameters and vice versa. The relationship between the ABCD transfer matrix is given as;

$$S_{12} = \frac{2}{A + B + C + D} \quad (1)$$

However, the generalized approximation for the filtering function is agreed upon as;

$$|S_{12}(j\omega)|^2 = \frac{1}{1 + \varepsilon^2 F_N^2(\omega)} \quad (2)$$

From (2), $F_N(\omega) = N^{\text{th}}$ order filtering function and, ε = ripple level. The overall transmission (ABCD) matrix of Path 1 is given in (3), which is obtained by multiplying the transfer matrix of all the cascaded sections, respectively.

$$[T]_{PATH1} = \begin{bmatrix} A_1 & B_1 \\ C_1 & D_1 \end{bmatrix}_{PATH1} = [T_{SIR}] \times [T_{OCS}] \times [T_{SIR}] \quad (3)$$

Where,

$$[T_{SIR}] = [T_1] \times [T_2] \times [T_1] \quad (4)$$

However, from Fig. 1, path 2 entails a straight transmission line. Therefore, the transmission matrix of a transmission line is represented in (5).

$$\begin{bmatrix} A & B \\ C & D \end{bmatrix} = \begin{bmatrix} \cos \theta & j Z_s \sin \theta \\ j \sin \theta / Z_s & \cos \theta \end{bmatrix} \quad (5)$$

Where, Z_s is the characteristics impedance and θ is the corresponding electrical length. The matrix (5) for the transmission line and its corresponding SIR structure are identical and may be employed with SIR configuration by interchanging it with two matrices for each SIR section. Using eq.3, the overall transmission matrix for Path 1 is as follows.

$$[T]_{PATH1} = \prod_{p=1}^2 \begin{bmatrix} \cos \theta & j Z \sin \theta \\ j \sin \theta / Z & \cos \theta \end{bmatrix} \times \begin{bmatrix} 1 & 0 \\ \sin \theta / -j Z_o \cos \theta & 1 \end{bmatrix} \quad (6)$$

The first and second matrices show the transfer function of two-step impedance resonators and open-circuit stubs, respectively. The relation (6) gives the transfer function for Path 1.

It has been seen from Fig. 1 that both paths 1 and 2 are parallel to each other. Therefore, it would be prudent to consider admittance (Y-parameter) instead of impedance. The Y-parameter matrix for Path 1 is evaluated from the ABCD transfer matrix (6) using the following set of parameters.

$$Y_{11} = \frac{D}{B} ; Y_{12} = \frac{(BC) - (AD)}{B} ; Y_{21} = -\frac{1}{B} ;$$

$$\& Y_{22} = \frac{A}{B}$$

Therefore, Y-matrix for Path 1 is written as.

$$[Y]_{PATH1} = \begin{bmatrix} Y_{11} & Y_{12} \\ Y_{21} & Y_{22} \end{bmatrix} \quad (7)$$

Subsequently, the generated Y-matrix for Path 2 may be written as;

$$[Y]_{PATH2} = \begin{bmatrix} -\frac{I \cos(2\theta)}{Z_s \sin(2\theta)} & -\frac{I(-\cos(2\theta)^2 - \sin(2\theta)^2)}{Z_s \sin(2\theta)} \\ I & -\frac{I \cos(2\theta)}{Z_s \sin(2\theta)} \end{bmatrix} \quad (8)$$

Using eq. 7 and eq. 8, $[Y]_{Filter}$ is obtained.

$$[Y]_{Filter} = [Y]_{PATH1} + [Y]_{PATH2} \quad (9)$$

Again, Y-parameters are converted to ABCD parameters. Using (1), the transmission coefficient is solved by putting in values of A, B, C, and D. In the next step, the filtering function is evaluated from the transmission coefficient by using (2). whereas (10) gives a general relation, which determines the order of a filter.

$$N = k + 3 \quad (10)$$

Where k = length factor of a step impedance. As given in Fig. 1, $k = 1$. On simplifying, the filtering function of the 4th order proposed filter is derived in (11). For the sake of simplicity, $\varepsilon = 1$.

$$F_4(\theta) = \frac{\alpha \cos^4 \theta + \beta \cos^3 \theta + \gamma \cos^2 \theta + \delta \cos \theta + \rho}{\sigma} \quad (11)$$

From above $\alpha = \gamma \neq 0$, so the extracted variables are given as under.

$$\alpha = \frac{-((z_s - 1)z - z_s)^2(z + 2z_0)^2((z_s + 1)z + z_s)^2}{z^2 z_0^2} \quad (12)$$

$$\beta = \frac{3((z_s - 1)z - z_s)(z_s^2 - 1)z^3 + \left(\frac{2}{3}z_0 z_s^2\right)z^2 - \frac{4}{3}z_s \left(\frac{z_0}{4}z_s\right)z - \frac{2}{3}z_0 z_s^2}{z^2 z_0^2} + 2z_0((z_s + 1)z + z_s) \quad (13)$$

$$\gamma = -\frac{\left(\begin{matrix} \left(\frac{4}{3}z_0 z_s^4 \right) z^3 + \frac{4}{3} \left(\begin{matrix} -\frac{1}{2}z_s^3 \\ -2z_0 z_s^2 + \left(\frac{8}{3}z_0^2 + \frac{2}{3} \right) z_s^3 \\ +4z_0 z_s^2 \end{matrix} \right) z^2 + \left(\begin{matrix} -\frac{4}{3}z_0 z_s^4 + \left(\frac{8}{3}z_0^2 + \frac{2}{3} \right) z_s^3 \\ +4z_0 z_s^2 \end{matrix} \right) z + \frac{4}{3}z_0 z_s^3 (z_0 z_s + 1) \end{matrix} \right)}{z_0^2} \quad (14)$$

$$\delta = \frac{z^4((z_s^4 + 1)z^2 + (4z_0 z_s^2 - 2z_s^3 + 2z_s)z + 4z_0 z_s^3 + z_s^2)}{z_0^2} \quad (15)$$

$$\rho = -\frac{z^4 z_s^2}{z_0^2} \quad (16)$$

Here, z, z_0 and $z_s > 0$. As the highest degree suggests in (11), it indicates that the maximum of four transmission poles can be achieved by choosing suitable characteristic impedances. From (11), θ can be solved as

$$\theta = \theta_{TZ} = \cos^{-1} \sqrt{\frac{-b \pm \sqrt{b^2 - 4ac}}{2a}} \quad (17)$$

$$f_{TZ} = \frac{\theta_{TZ}}{\theta_0} f_0 \quad (18)$$

Where (18) gives the relation between frequency and electrical length. From (11), the filtering function can be approximated to Chebyshev polynomial Type-I to evaluate electrical parameters. By substituting characteristics impedance and electrical length values of $Z_{in} = 77.2 \Omega$, $\theta_{in} = 90^\circ$, $Z_2 = 90 \Omega$, $\theta_s = 50.5^\circ$. As the model indicates, the twin SIRs are connected with a half-wavelength transmission line having impedance $Z_1 = 59.74 \Omega$ and electrical length $\theta_1 = 23.3^\circ$. Whereas a quarter wavelength open-circuit stub (OCS) is represented as a resonator with characteristic impedance $Z_s = 43.04 \Omega$ and $\theta_s = 50.5^\circ$ respectively.

The frequency response shown in Fig.2 reveals that two stopbands are achieved with a rejection level of greater than 58.5 dB. whereas seven transmission poles ensure the good electrical performance of a proposed design. Furthermore, the coefficients α, β, γ & ρ provided concerning 12-18, shifts the position of transmission poles (TPs) peak values. The superposition of the total electrical length of path 1 and path 2 leads to dual-stopbands at desired frequencies.

C. Analysis of Proposed Filter

This section discusses the effect on the frequency concerning changes in the path 1 open stub resonator's electrical length. The open stub has an electrical length of 50.5° . The

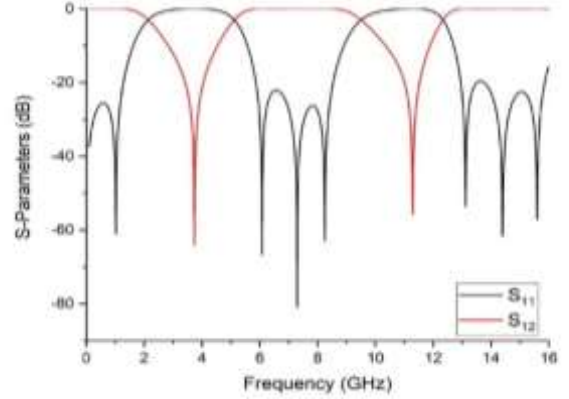


FIGURE 2: Response of ideal transmission Model

corresponding result shows that decreasing the electrical length produces a right shift in TZs. Increasing the electrical length produces a left shift in TZs. The variations in TZs frequency are represented in Fig.3, respectively. However, a considerable shift in TZs is observed in the second stopband of the dual-bandstop result.

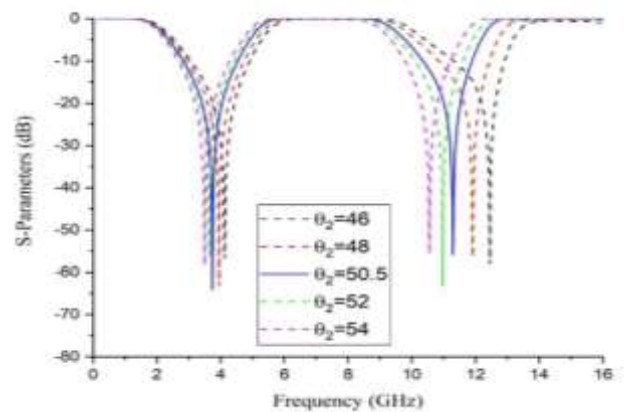


FIGURE 3: Effect on TZs by varying electrical length

III. RESULTS AND MEASUREMENTS

For the actual response of the proposed design, the circuit is designed using microstrip transmission lines (TLs). Due to parasitic losses, the performance of DBBSF is changed compared to the ideal circuit's response. Due to good dielectric properties and available resources, Roger Duriod RT/5880 substrate is engaged in realizing the proposed DBBSF. In microstrip design, physical parameters are extracted using electrical parameters from the ideal design. Due to the lossless nature of ideal design, microstrip-based design is important to overcome the losses incurred in the ideal design. The designed filter has symmetrical stepped-impedance resonators which are separated by an open circuit stub w_3 mm, $l_6/2$ mm. The symmetric SIRs also contain an MSTEP line which is nothing, just a variant of widths w_6 and w_2 . Whereas the two SIRs connect with the main microstrip transmission line at w_1 and L (l_1+w_3). However, the physical parameters in width and length of step, open stub, and main transmission line are provided using line calculator in Advanced Design System (ADS) $w_{in} = 2.97012$, $l_{in} = 6.57372$, $w_1 = 0.8876$, $l_1 = 12.3762$, $w_2 = 0.505508$, $l_2 = 13.7677$, $w_3 = 2.3725$ and $l_3 = 7.0858$. All the units are in 'mm'. As illustrated in Fig.4, the superposition of signals generates six TPs located at $f_{TP_1} = 5.58\text{GHz}$, $f_{TP_2} = 7.4\text{ GHz}$, $f_{TP_3} = 9.4\text{ GHz}$, $f_{TP_4} = 12.47\text{ GHz}$, $f_{TP_5} = 13.39\text{ GHz}$, and $f_{TP_6} = 15.71\text{ GHz}$. However, the in-band insertion loss of each stopband is greater than 20 dB. In addition to that four TZs are obtained at $f_{TZ_1} = 3.54\text{ GHz}$, $f_{TZ_2} = 3.94\text{GHz}$, $f_{TZ_3} = 10.79\text{ GHz}$, $f_{TZ_4} = 11.35\text{ GHz}$ respectively.

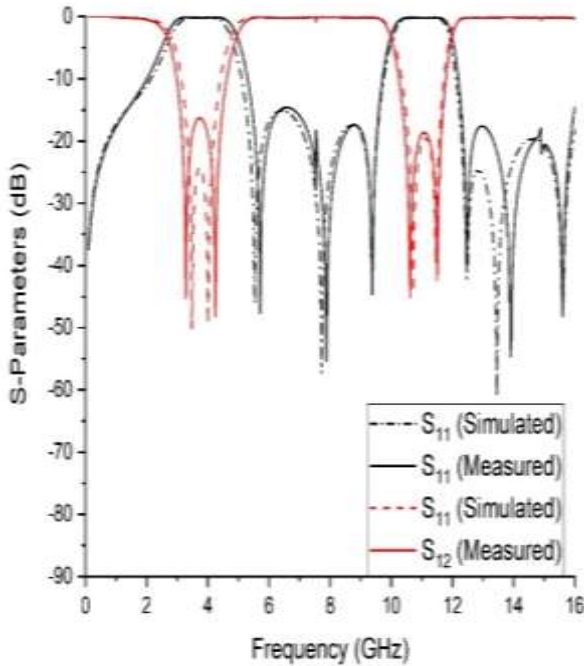


FIGURE 4: Simulated and measured S-parameters response

It has been measured that the first stopband has 3-dB bandwidth from 2.53 GHz to 4.91 GHz. Whereas the second stopband has 3-dB bandwidth from 10.14 GHz to 11.94 GHz, respectively. However, their centre frequencies are measured at 3.72 GHz and 10.77 GHz, respectively. It has also been observed that the minimum measured insertion loss (IL) at the first centre frequency is 29.1 dB. Whereas the measured IL at the second centre frequency is 24.07 dB, respectively.

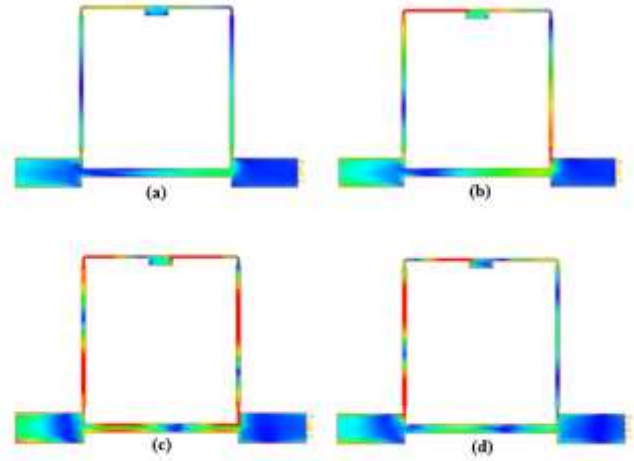


FIGURE 5: Current distribution across the proposed resonant structure at (a) 3.3GHz (b) 3.6 GHz (c) 10 GHz (d) 11.6 GHz resonant peaks

The tested prototype obtained TZs at 3.6, 3.93, 10.85, and 11.36 GHz, respectively. To understand the mechanism of EM wave transmission, the current distribution has also been analyzed in the proposed structure of DBBSF. For this reason, the current distribution of the resonant structure in both stopbands of resonant peaks is illustrated in Fig. 5. The result demonstrates that in the 1st stopband, the symmetrical distribution of current takes place along the left and right sides at 3.5GHz and 3.9GHz. Whereas in another response, the symmetrical distribution of current is shown for the 2nd stopband located at resonant peaks of 10.7 GHz & 11.39 GHz.

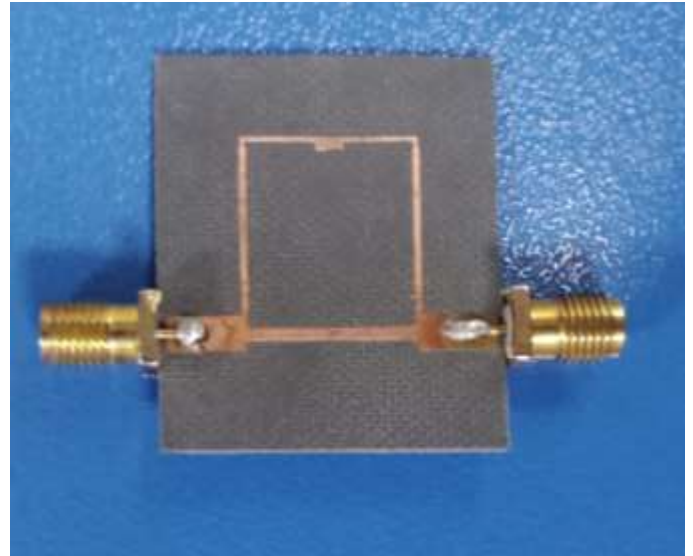


FIGURE 6: Simulated and measured S-parameters response

The results have depicted that a strong electrical resonance occurs when the symmetrical distribution of currents across the structure takes place. When the frequency of the input EM wave is identical to the resonant frequency, practically all EM wave energy may be utilized to maintain the electron oscillation due to the strong resonant. When the incoming EM wave's frequency is not the resonant frequency, however, practically all of the energy flows through the device. Table I

below shows the comparison with previously designed dual-band bandstop filters.

Table I: Comparison with different discussed topologies

Ref.	CF's (GHz)	TPs, S ₁₁	TZs, S ₁₂	Circuit Size, ($\lambda_g \times \lambda_g$)
[14]	1/1.9	3	3	Not given
[15]	1.5/3.16	3	2	0.44 x 0.37
[16]	9.8/11.4	1	3	Not given
[17]	1.5/3.15	4	2	1.09 x 0.70
[18]	2.69/2.86	2	2	0.30 x 0.26s
[19]	1.16/3.5	4	5	Not given
[20]	3.8/5.3	3	4	0.201 x 0.101
[21]	1.7/5	7	4	Not given
[22]	1.8/5.2	2	2	0.29 x 0.13
[23]	1.5/2.4	9	9	0.65 x 0.38
This paper	3.76/11.04	7	4	0.52x0.33

It is easy to observe that the proposed bandstop filter has performed better than the compared topologies. Thus providing a low insertion loss, compact size, and greater number of transmission zeros. It is also noticeable that the proposed topology is very simple and easy to fabricate. The fabricated DBBSF is shown in Fig. 6.

IV. CONCLUSION

This paper presents an explanation of a highly selective dual-band bandstop filter that is based on dual-path SIR. A dual-band BSF is produced by the design that is being proposed, and its fractional bandwidths are 50.5% and 16.36% at 3.76 and 11.04 GHz, respectively. The theoretical concepts and analysis were validated through the construction and testing of a prototype. The proposed dual-band BSF is a viable option for contemporary wireless communication systems thanks to its adaptable design and high out-of-band insertion.

FUNDING STATEMENT

The author(s) received no specific funding for this study.

CONFLICTS OF INTEREST

The authors declare they have no conflicts of interest to report regarding the present study.

REFERENCES

[1] P. Chen, L. Li, K. Yang, K. Hua and X. Luo, "A microstrip dualband bandstop filter with dualband bandstop resonators," *2017 IEEE 17th International Conference on Communication Technology (ICCT)*, Chengdu, 2017, pp. 1685-1688, doi: 10.1109/ICCT.2017.8359917.

[2] H. G. Alrwuili and T. S. Kalkur, "A novel compact dual-band bandstop filter (DBBSF) using spurline & stepped-impedance resonator with a tunable BST capacitors," *2017 Joint IEEE International Symposium on the Applications of Ferroelectric (ISAF)/International Workshop on Acoustic Transduction Materials and Devices*

(IWATMD)/Piezoresponse Force Microscopy (PFM), Atlanta, GA, 2017, pp. 9-14, doi: 10.1109/ISAF.2017.8000199.

[3] S. J. Xue, H. T. Zhu, W. J. Feng and W. Q. Che, "Dual-wideband bandstop filter using transversal signal-interaction concept," in *Electronics Letters*, vol. 49, no. 9, pp. 604 -605, 25 April 2013, doi: 10.1049/el.2012.4312.

[4] Z. Jiang, Z. Sun, Y. Li and Y. Zhao, "A wide dual band stop-band filter with two different defected microstrip structures," *2017 Progress in Electromagnetics Research Symposium - Fall (PIERS - FALL)*, Singapore, 2017, pp. 1997-2000, doi: 10.1109/PIERS-FALL.2017.8293465.

[5] X. Zheng, H. Wang and Y. Sun, "Analysis of microstrip bandstop filter characteristic based on defected microstrip structure," *2017 Progress In Electromagnetics Research Symposium - Spring (PIERS)*, St. Petersburg, 2017, pp. 704-707, doi: 10.1109/PIERS.2017.8261833.

[6] F. Chen, N. Zhang, P. Zhang and Q. Chu, "Design of ultra-wideband bandstop filter using defected ground structure," in *Electronics Letters*, vol. 49, no. 16, pp. 1010-1011, 1 Aug. 2013, doi: 10.1049/el.2013.1541.

[7] M. Rao, Y. Wu, W. Wang, and Y. Liu, "Design of Compact Wideband High-Selectivity Band-Stop Filter Based on Coupled Lines," *Progress In Electromagnetics Research C*, vol. 53, pp. 55-66, 2014.

[8] P. Castillo-Aranibar, A. Garca-Lampérez, S. Llorente-Romano and D. Segovia-Vargas, "Dual-band band-stop microstrip filter with controllable bands based on unequal split ring resonators," in *IET Microwaves, Antennas & Propagation*, vol. 13, no. 12, pp. 2119-2128, 2 10 2019, doi: 10.1049/iet-map.2018.5926.

[9] W. J. Feng, M. L. Hong, W. Q. Che and Q. Xue, "Dual-Band Microstrip Bandstop Filter With Multiple Transmission Poles Using Coupled Lines," in *IEEE Microwave and Wireless Components Letters*, vol. 27, no. 3, pp. 236-238, March 2017, doi: 10.1109/LMWC.2017.2661704.

[10] W. Wang, M. Liao, Y. Wu and Y. Liu, "Small-size high-selectivity bandstop filter with coupled-line stubs for dual-band applications," in *Electronics Letters*, vol. 50, no. 4, pp. 286-288, 13 February 2014, doi: 10.1049/el.2013.3704.

[11] Y. Cai, K. D. Xu, Z. Ma and Y. Liu, "Compact bandstop filters using coupled lines and open/short stubs with multiple transmission poles," in *IET Microwaves, Antennas & Propagation*, vol. 13, no. 9, pp. 1368-1372, 24 7 2019, doi: 10.1049/iet-map.2018.5745.

[12] S. Yang, "Simulation of a compact dual-band microstrip bandstop filter having three spurlines," *SoutheastCon 2016*, Norfolk, VA, 2016, pp. 1-3, doi: 10.1109/SECON.2016.7506741.

[13] A. C. Guyette and E. J. Naglich, "Short-Through-Line Bandstop Filters Using Dual-Coupled Resonators," in *IEEE Transactions on Microwave Theory and Techniques*, vol. 64, no. 2, pp. 459-466, Feb. 2016, doi: 10.1109/TMTT.2015.2506631.

[14] C.-K. Lung, K.-S. Chin, and J. S. Fu, "Tri-section stepped-impedance resonators for design of dual-band bandstop filter," in *Proc. Eur. Microw. Conf. (EuMC)*, Oct. 2009, pp. 771-774.

[15] C.-H. Tseng and T. Itoh, "Dual-band bandpass and bandstop filters using composite right/left-handed metamaterial transmission lines," in *2006 IEEE MTT-S International Microwave Symposium Digest*, 2006, pp. 931-934.

- [16] K.-S. Chin, J.-H. Yeh, and S.-H. Chao, "Compact Dual-Band Bandstop Filters Using Stepped-Impedance Resonators," *IEEE Microw. Wirel. Compon. Lett.*, vol. 17, no. 12, pp. 849–851, Dec. 2007.
- [17] S. Fallahzadeh, H. Bahrami, and M. Tayarani, "A novel dual-band bandstop waveguide filter using split ring resonators," *Prog. Electromagn. Res. Lett.*, vol. 12, pp. 133–139, 2009.
- [18] J.-K. Xiao and H.-F. Huang, "Square patch resonator bandstop filter," in *Communication Technology (ICCT), 2010 12th IEEE International Conference on*, 2010, pp. 104–107.
- [19] L. Gao, S. W. Cai, X. Y. Zhang, and Q. Xue, "Dual-band bandstop filter using open and short stub-loaded resonators," in *Microwave and Millimeter Wave Technology (ICMMT), 2012 International Conference on*, 2012, vol. 4, pp. 1–3.
- [20] J. Wang, H. Ning, L. Mao, and M. Li, "Miniaturized dual-band bandstop filter using defected microstrip structure and defected ground structure," in *Microwave Symposium Digest (MTT), 2012 IEEE MTT-S International*, 2012, pp. 1–3.
- [21] S. Majidifar, S. V. A.-D. Makki, S. Alirezaee, and A. Ahmadi, "Dual-band bandstop filter using modified stepped-impedance hairpin resonators," in *Proc. 5th Int. Conf. Comput. Intell. Commun. Netw.*, Sep. 2013, pp. 61–63.
- [22] A. Joshi and D. Bhatia, "Analysis and design of compact dual-band bandstop filter using E-shaped resonators," in *2014 International Conference on Advances in Engineering & Technology Research (ICAETR - 2014)*, 2014, pp. 1–3.
- [23] W. J. Feng, M. L. Hong, W. Q. Che, and Q. Xue, "Dual-Band Microstrip Bandstop Filter With Multiple Transmission Poles Using Coupled Lines," *IEEE Microw. Wirel. Compon. Lett.*, vol. 27, no. 3, pp. 236–238, Mar. 2017.
- [24] Hunter, Ian. *Theory and design of microwave filters*. No. 48. Iet, 2001.